

CONSTITUTIVE MODELS FOR SUBSOIL IN THE CONTEXT OF STRUCTURAL ANALYSIS IN CONSTRUCTION ENGINEERING

T. Knabe*

* *Graduiertenkolleg 1462*
Bauhaus-Universität Weimar
Berkaerstr. 9
99425 Weimar
E-mail: tina.knabe@uni-weimar.de

Keywords: Clay, Identification, Optimization, Structures

Abstract. *Parameters of constitutive models are generally obtained by comparing the results of forward numerical simulations to measurement data. Mostly parameter values are varied by trial-and-error in order to reach an improved fit and to obtain plausible results. However, the description of complex soil behavior requires advanced constitutive models where the increasing complexity of these models mainly increases the number of unknown constitutive parameters. Thus an efficient identification "by hand" becomes quite difficult for most practical problems. In this paper an iterative approach is present to determine the material parameters for different clays. Furthermore the influence of destructuring, anisotropy, consolidation, creep and soon is investigated by different complex constitutive models for clay. Finally, a statistical assessment is carried out of numerical results to evaluate different constitutive models. Additionally a geotechnical problem, stone columns under an embankment, is treated in a well instrumented field trial in Klagenfurt, Austria. For the identification purpose there are measurements from multilevel-piezometers, multilevel-extensometers and horizontal inclinometers. Based on the simulation of the boundary problem "stone columns" in a FE-Model the identification of the constitutive parameters is similar to the experimental tests by minimizing the absolute error between measurement and numerical curves.*

1 INTRODUCTION

Many constitutive models for clay can be found in literature [1]. Each model is different in complexity and in number, importance and determinability of the involved constitutive parameter. With an increasing number of constitutive parameters it becomes more difficult to determine parameters from laboratory or field tests. Furthermore many different tests, with different stress paths and initial conditions on reconstituted or natural specimen, are necessary to devise realistic parameters for the constitutive models. For the computation of realistic problems, in addition to a physical correct modeling of the material behavior, all parameters of the applied material model for a specific material must be known. As a consequence of the complexity of the applied material model, a direct experimental determination of the material parameters is often not possible.

Due to this situation an iterative approach is needed to determine the constitutive parameters. In the following, a population-based procedure is used. Hence this study concerns the identification of the parameters of constitutive models from standard geotechnical laboratory and field tests.

2 CONSTITUTIVE MODELS FOR CLAY

The constitutive models, which are available, are presented in hierarchical order; starting from simple ideal elastic, ideal plastic constitutive models to assorted hardening and softening multi surfaces models.

2.1 Mohr-Coulomb model

The Mohr-Coulomb model (MC) is the classical elasto-plastic model with a fixed yield surface in principal stress space, which is not affected by plastic straining [2]. Additionally Hooke's law is used to relate the stress rates to the elastic strain rates (see Fig. 1). The model

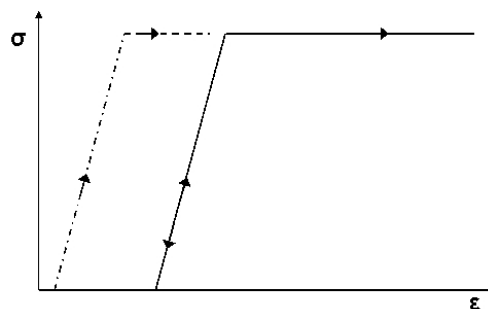


Figure 1: Basic idea of an elastic perfectly plastic model

includes the Mohr-Coulomb failure criterion, which describes a linear relation between normal and shear stresses at failure.

For the Mohr-Coulomb model only five constitutive parameters (Young's modulus E , poisson's ratio ν , friction angle φ , cohesion c and dilatancy angle ψ) are needed to describe the soil behavior. These parameters can be determined from the results of standard geotechnical testing.

2.2 Soft Soil Creep model

The Soft Soil Creep model (SSC) is a viscoplastic model incorporating time dependent behavior [3]. The total strains consists of a time independent elastic part and a time dependent viscoplastic part. The ultimate failure criterion is based on Mohr-Coulomb. An elliptical cap

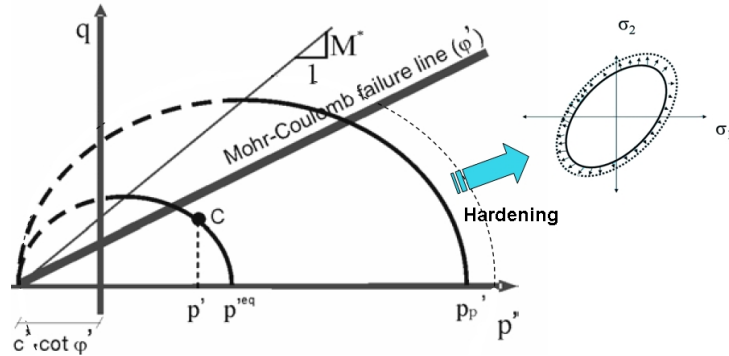


Figure 2: Soft Soil Creep model: Yield curve and hardening in principle stress space according to [3]

is introduced, which shape is controlled by the slope of the critical state line. The size of the cap changes due to accumulated volumetric viscoplastic creep strains ϵ_v^{vp} . The parameters in the SSC model (modified compression index λ^* , modified swell index κ^* , modified creep index μ^* , φ , c , positions's ratio ν and ψ) can be determined from standard triaxial and oedometer tests with time measurement.

2.3 S-CLAY1 models

The S-CLAY1 model is an elasto-plastic model, which accounts for plastic anisotropy [1] for normally or lightly overconsolidated clays. An extension, which takes destructuration into account (S-CLAY1S model) is described by Koskinen et al. 2002 [4]. To do so an "intrinsic yield surface", IYS, is introduced. The IYS refers to equivalent unbounded soils having the same shape and orientation at the same void ratio within the yield surface. Using an initial inclination of the yield surface α_0 anisotropy is considered for the plastic behavior which is a sheared ellipsoid in the principal stress space (see Fig.3). The initial inclination of the yield surface α_0 can be related to the earth pressure factor at rest K_0^{NC} , which can in return be related to the friction angle φ (e. g. by [5]). The additional constitutive parameter for anisotropy and destructuration of the S-CLAY1S models are summarized in Table 1. They cannot be determined from standard laboratory tests.

Table 1: Model parameter for the S-CLAY1S model

Parameter	Comment
α_0 : Initial size and inclination of the yield curve	Anisotropy: Estimated via φ'
μ : Absolute effectiveness of rotational hardening	Anisotropy: typical values: $10/\lambda - 20/\lambda$
β : Relative effectiveness of rotational hardening	Anisotropy: Estimated via φ'
x_0 : Initial bonding effect	Destructuration: S_t-1
a : Absolute effectiveness of destructurational hardening	Destructuration: typical values: 8-11
b : Relative effectiveness of destructurational hardening	Destructuration: typical values: 0.2-0.3

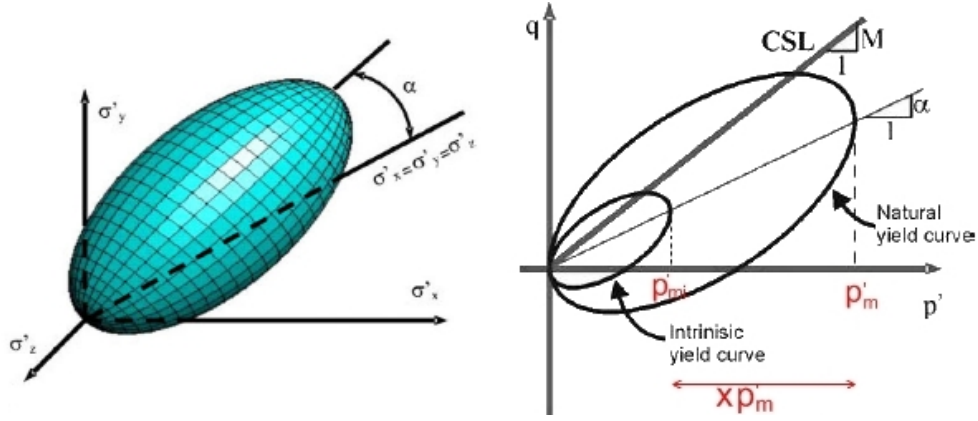


Figure 3: S-CLAY 1S model: yield curve according to [1] (a) 3D-stress space (b) in principle stress space

2.4 Multilaminate Model for Structured Clay

The Multilaminate Model (ML) for Structured Clay was developed by Galavi 2007 [6] and is based on the Multilaminate framework [7]. Anisotropy, destructuration and softening can be taken into account. The deformation behavior of the soil is obtained by integrating the response of an infinite number of randomly oriented "sampling planes". Each stress integration point is associated with a certain number of sampling planes with different orientations. The stress strain relations are formulated locally on a microscopic level, except for the elastic part, which is calculated at the macroscopic level. The global strains are obtained by numerical integration of the inelastic contribution from each sampling plane and the global elastic contribution. Hence, induced anisotropy can be considered without extra material parameters. In order to

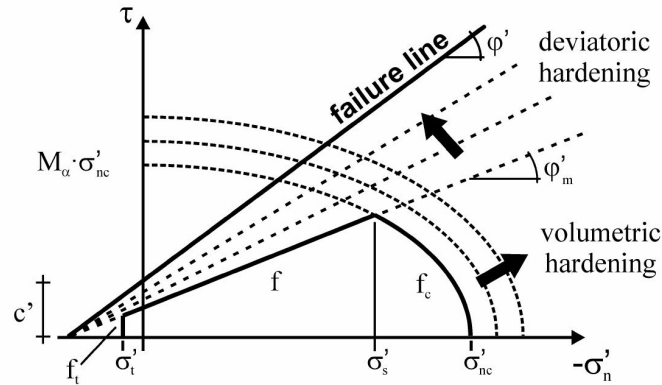


Figure 4: Multilaminate model: yield curve and hardening [6]

include the inherent anisotropy, a so-called micro structure tensor (Pietruszczak & Mroz 2000) [8] is implemented. To take destructuration into account, it is assumed, that it starts at gross yield. Destructuration is related to the damage strain ϵ_{di} , where an increase in strain leads to an decrease in structure and depends on a bonding parameter b and the volumetric rate of the destructuration h_v .

$$\epsilon_{di} = (1 - A_d)\epsilon_{n,i}^p + A_d\epsilon_{\gamma,i}^p \quad (1)$$

where $\epsilon_{n,i}^p$ the plastic normal strains from all parts of the yield curve, $\epsilon_{\gamma,i}^p$ are the plastic shear strains from all parts of the yield curve and A_d the parameter controlling the relative proportion of distortional and volumetric degradation.

$$\frac{db}{b} = -hd\epsilon_{di} \quad (2)$$

The additional constitutive parameters describing anisotropy and destructuration of the Multilaminate Model for Structured Clay are summarized in Table 2. Not all parameters can be determined by standard laboratory tests.

Table 2: Model parameter for the Multilaminate Model for Structured Clay

Parameter	Comment
$\sigma_{nc,i}$: Initial preconsolidation stress	Oedometer test
A_d : Parameter for proportion of plastic strains	Destructuration and anisotropy: 0-1
A_r : Anisotropy ratio	Anisotropy
b_0 : Size initial value of bonding	Destructuration: $\frac{\sigma'_{vy}}{\sigma'_{vy*}} - 1$
h_v : Volumetric rate of destructuration	Destructuration: typical values 10 – 30

2.5 Comparison of the different constitutive models

A overview of the constitutive models is presented in Table 3. It can be seen, that the models are very different in their complexity. Furthermore no model can consider all physical phenomena. Generally the number of the constitutive parameter increases with each phenomena incorporated into the model.

Table 3: Comparison different constitutive models

Name	Parameter	Hardening laws	Creep	Anisotropy	Destructuration	Softening
Mohr-Coulomb	5	-	no	no	no	no
SSC	8	1	yes	no	no	no
S CLAY 1S	12	3	no	yes	yes	no
Multilaminate	>15	3	no	yes	yes	yes

3 LABORATORY TESTING AND NUMERICAL MODELING

3.1 Oedometer and Triaxial tests

In order to get the properties of the soil laboratory tests are necessary. Normally these are oedometer (e. g. stress oder strain controlled) and triaxial (e. g. drained, undrained) tests.

To verify the identification procedure four different clays with different behavior and characteristics are investigated. These are namely clays found in Bothkennar (Scotland) (for example well described in (*Géotechnique Symposium-in-Print*, 1992), Pisa (Italy) (see such as [9] for details) and StCesaire (Canada) [10], which are very soft clays, and Pappadai Clay, which is a stiff clay from Italy [11, 12].

3.2 Measurement errors

According to Baldi [13] errors occurring in laboratory testing could be seating errors, alignment errors, bedding errors or compliance errors.

These errors vary with different types of tests, age of test apparatus, stress level, etc. and will be taken into account in the statistical assessment. An example will be given for oedometer and triaxial test apparatus, which was used by Sukolrat [14] for testing Bothkennar Clay (Table 4).

Table 4: Measurement errors

Apparatus	Measurement	Error	σ_ϵ
Oedometer	Displacements	± 0.02 mm	0.001
	Load	± 3 N	
Triaxial	Pressure	± 0.2 kPa	
	External displacements	± 0.05 mm	0.001
	Internal displacements	± 0.005 μm	

3.3 Simulation

All tests are simulated as element tests in a Finite-Element-program.

In a first step the simulations were done by using values from literature (e. g. Bothkennar Clay [14, 15, 16]). The simulation results of an oedometer test on reconstituted Bothkennar Clay (OED4B) with loading and unloading are shown in Fig.5. It can be recognized, that the "simple" Mohr-Coulomb model is unable to represent the observed non-linear stress-strain behavior. The SSC, S-CLAY1S and the ML model underestimate the vertical strains to a greater or lesser extent.

4 OPTIMIZATION

Due to the unsatisfying results obtained with the values from literature a back analysis in terms of direct or inverse approaches can be used to calibrate the material model parameters [17]. In this article the direct approach is used which is based on an iterative procedure correcting the trial values of the unknown parameters p by minimizing the objective function. The material parameters are the unknowns and the objective function consists of the difference between measured and simulated data.

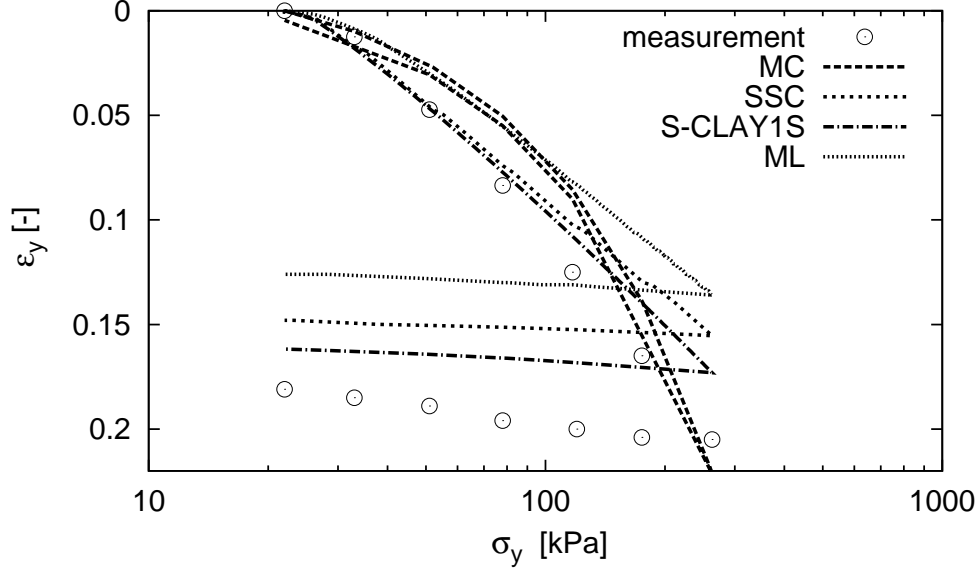


Figure 5: Observed and simulated vertical strain of an triaxial test on reconstituted Bothkennar Clay with parameters from the literature (according to [14])

The objective function reads:

$$F(p) = \sqrt{\frac{\sum_{i=1}^n f_{i(p)}^2 \cdot w_i}{\sum_{i=1}^n y_{i,meas}^2}} \quad \text{with} \quad f_{i(p)} = (y_{i,meas} - y_{i,calc(p)}) \quad (3)$$

where w_i are weighting factors and $i = 1, \dots, n$ is the counter of loading steps used in optimization process. In this article the particle swarm optimizer (PSO) is used to minimize the objective function [18].

The PSO approach is based on a population of individuals. Each particle represents a solution to the optimization problem. While searching for optima, each particle adjusts its trajectory according to its own previous best position, and the best previous position attained by any member of its neighbors. PSO starts by randomly initializing a population of individuals in the search space. The searching for the best solution then continues with particles changing through successive generations according to rules until a end-criterion is achieved.

4.1 Optimization Results

In this section examples of identification for different types of clays, phenomenas, tests and number of tests are presented.

4.1.1 Oedometer test on reconstituted Bothkennar Clay

For an oedometer test on reconstituted Bothkennar Clay (OED4B) the results of the optimized simulations for different constitutive models are shown in Fig.6. The simulated stress-strain behavior for the advanced soil models (SSC, S-CLAY1S, ML) results in a good agreement with the measurements. Due to its unrealistic physical structure it is not possible to improve the simulation of the MC model.

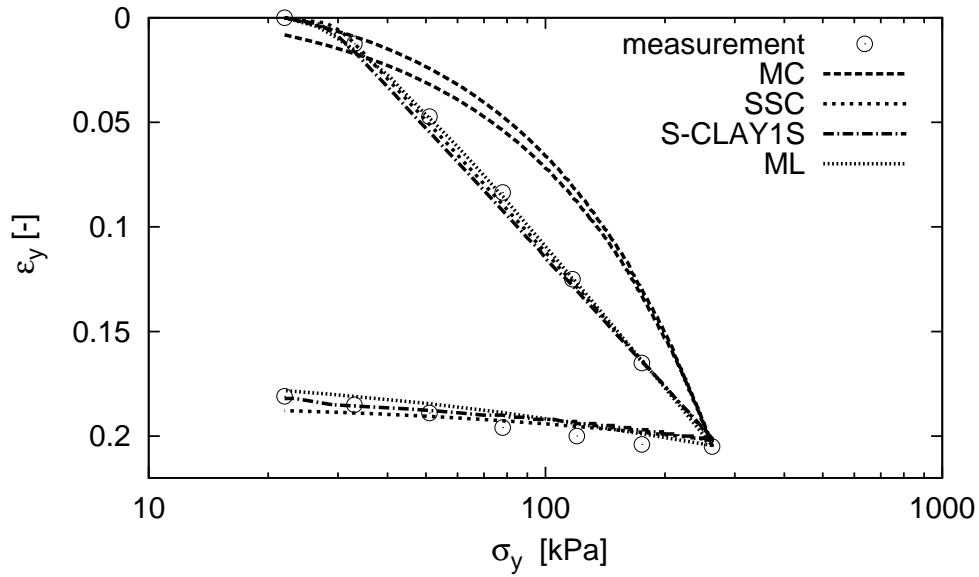


Figure 6: Observed and simulated vertical strain of an oedometer test on reconstituted Bothkennar Clay with optimized parameters (according to [14])

4.1.2 Triaxial test on natural Bothkennar Clay

The same identification procedure is done for a drained triaxial test on a natural sample of Bothkennar Clay. Figure 7 shows, that the "simple" MC model is also unable to predict the soil behavior in triaxial conditions properly. The SSC, S-CLAY1S and the ML models match the shape of the loading and the unloading paths well.

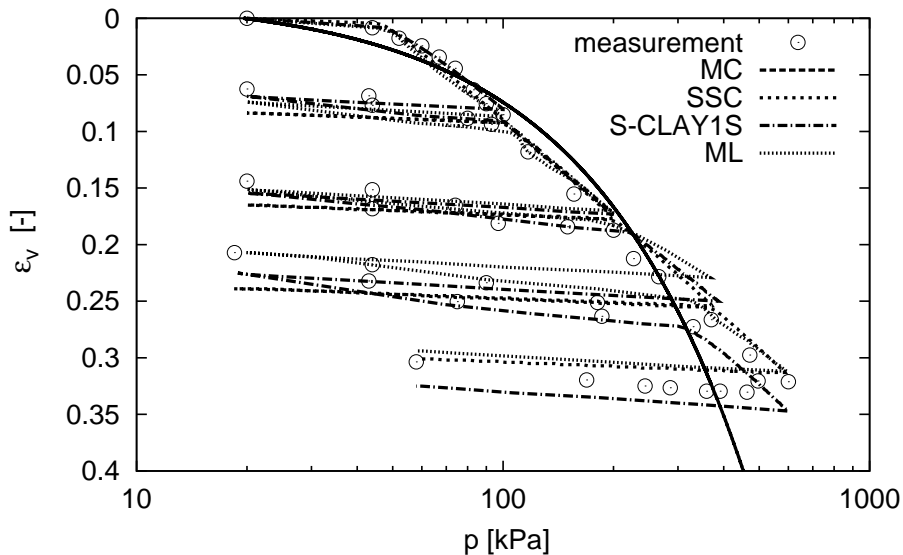


Figure 7: Observed and simulated vertical strain of a triaxial test on natural Bothkennar Clay with optimized parameters (according to [14])

4.1.3 Two different oedometer test

In a first step the oedometer tests are optimized separately. In a second step all tests are identified simultaneously. The results can be seen, for example, for two different oedometer tests on reconstituted Bothkennar Clay from a depths between 7.75 m and 8.1 m (separately: OED4A [19] and OED4B [section 4.1.1]) in Fig.8. Inspection of Figure 8 shows that by si-

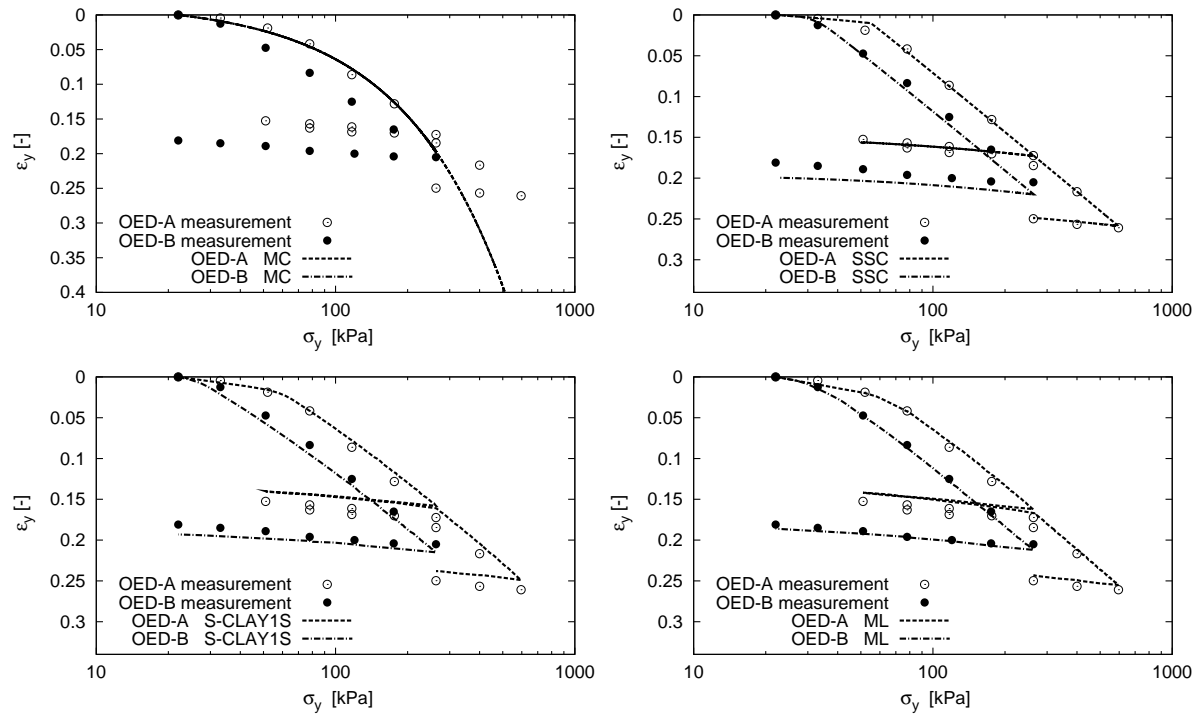


Figure 8: Observed and simulated vertical strain of two different oedometer tests on reconstituted Bothkennar Clay with optimized parameters (a) MC (b) SSC (c) S-SCLAY1S (d) ML (according to [14])

multaneous identification the results are less coincident, compared to a separated optimization. This result can be attributed to sampling disturbance and measurement errors, which yield to a light divergence of the stress-strain behavior in oedometric conditions.

5 STATISTICAL ANALYSIS

A statistical assessment is done after every optimization to determine the quality of the "curve fitting". In the next section an example is given to clarify the procedure for an oedometer test on reconstituted Bothkennar Clay.

5.1 Estimation of the accuracy of identified parameters

For this analysis equivalent errors for all measurement points (4) of a single test are assumed. The resulting covariance matrix can be written

$$\mathbf{C}_{\mathbf{X}\mathbf{X}} = \sigma_{\epsilon}^2 \cdot \mathbf{I} \quad (4)$$

where σ_ϵ^2 is the strain measurement error and \mathbf{I} is the unit matrix. According to [20] we estimate the parameter covariances as follows

$$\mathbf{C}_{pp} = (\mathbf{A}^T \mathbf{C}_{XX}^{-1} \mathbf{A})^{-1} = \sigma_\epsilon^2 (\mathbf{A}^T \mathbf{A})^{-1} \quad (5)$$

where $\mathbf{A} = \partial \mathbf{x} / \partial \mathbf{p}$ is the sensitivity matrix. The corresponding standard deviations of the parameters are obtained from the diagonal elements of the parameter covariance \mathbf{C}_{pp} .

By the estimation of the parameters for the oedometer test on reconstituted Bothkennar Clay (OED4B) it is not possible to calculate the covariance \mathbf{C}_{pp} of all parameters for the MC model, because the sensitivities of friction angle and cohesion are very low. Due to this nearly linearly dependent entries in the matrix $\mathbf{A} \mathbf{A}^T$ occur which is therefore not stable invertible. The Young's modulus and the shear modulus respectively for the MC model can be identified most reliable, followed by the poisson's ratio. For the SSC, S-CLAY1S and ML model the (modified) compression and (modified) swell index can be identified most reliable (see Table 5 - 7).

Table 5: Parameter covariance \mathbf{C}_{pp} for the SSC model (Oedometer test on reconstituted Bothkennar Clay (OED4B))

κ	λ	ν	φ	\mathbf{c}
0.0013493	-1.116E-05	-0.0495492	0.0244494	-0.4955941
-0.0006139	0.0005667	0.0289102	-0.015749	0.3767757
-0.0495493	0.0289102	2.0618492	-1.0135953	21.563505
0.0244494	-0.0157490	-0.0495493	0.5520917	-11.752265
-0.4955941	0.3767760	21.563505	-11.752265	265.4526

Table 6: Parameter covariance \mathbf{C}_{pp} for the S-CLAY1S model (Oedometer test on reconstituted Bothkennar Clay (OED4B))

κ	ν	λ	M	μ	β	α_0
0,04172	-3,3657	-3,02E-08	19,532	-1075	64,279	-0,42019
-3,3657	3802	1,43E-06	-17840	776677	-52111	-922,4
-3,02E-08	1,43E-06	9,58E-09	-6,83E-06	0,000363	-2,49E-05	5,65E-07
19,532	-17840	-6,83E-06	84532	-3694834	246945	4348
-1075	776677	0,000363	-3694834	163283732	-10863686	-177494
64,27	-52111	-2,49E-05	246945	-10863686	724587	12146
-0,42019	-922,4	5,65E-07	4348	-177494,	12146	322,67

5.2 Residual analysis

For the correct realistic model the residuals are independent and normally distributed with zero mean value. The mean value, standard deviation and skewness were computed to assess the normality of the residuals and the quadratic correlation coefficient with respect to the measurement point in order to evaluate their independence [21]. The mean value μ is defined as

$$\mu = \frac{1}{n} \sum_{i=1}^n x_i \quad (6)$$

Table 7: Parameter covariance C_{pp} for the ML model (Oedometer test on reconstituted Bothkennar Clay)

λ	κ	ν	φ	A_r	A_d	c
0,0027	0,017455	-0,0371	1,438	-0,9876	1,21E+11	0,89884
0,0174	0,182678	-0,5532	8,993	-14,84	2,29E+12	26,73
-0,0372	-0,55325	3,088	-15,63	43,58	-9,93E+12	-46,47
1,438	8,993	-15,636	878,7	-16,91	5,52E+13	-2017,
-0,9876	-14,841	43,58	-16,910	4189	-1,23E+14	-17799
1,21E+11	2,29E+12	-9,93E+12	5,524E+13	-1,23E+14	1,49E+26	-2,99E+13
0,89884	26,738	-46,47	-2017	-17799	-2,99E+13	86589

where n are the number of samples and x_i is any individual sample in a set of data. The standard deviation σ is the positive square root of the variance and calculated by

$$\sigma = \sqrt{\frac{1}{n} \sum_{i=1}^n (x_i - \mu)^2}. \quad (7)$$

The skewness γ_1 , the third standardized moment, is written as

$$\gamma_1 = \frac{\mu_3}{\sigma^3} \quad (8)$$

where μ_3 is the third moment about the mean. A negative skew is called *left-skewed*, i. e. the data are skewed left and a positive skew indicates data that are skewed right (*right-skewed*). The skewness of a normal distribution is zero.

The quadratic coefficients of correlation are defined by

$$\rho_{ij} = \frac{1}{n-1} \frac{\sum_{k=1}^n (\hat{y}^{(k)}(x_i) - \mu_{\hat{y}(x_i)}) (x_j^{(k)} - \mu_{x_j})}{\sigma_{\hat{y}(x_i)} \sigma_{x_j}} \quad (9)$$

where $\hat{y}(x_i)$ is the quadratic regression. A correlation greater than 0.7 is generally described as strong, whereas a correlation less than 0.3 is generally described as weak.

The results for the oedometer test on reconstituted Bothkennar Clay (OED4B) are given in Table 8 together with the final objective function values.

Obviously the SSC, S-CLAY1S and the ML model are able to simulate the stress-strain behav-

Table 8: Residual analysis for the oedometer test on reconstituted Bothkennar Clay

Models	Mean value	Standard Deviation	Skewness	Correlation	Objective function
MC	0.071378	0.0701863	0.349232	0.7314	1.109
SSC	-0.0004039	0.00392825	-0.0217733	0.6273	0.7202
S-CLAY1S	0.0005574	0.00506183	-0.496652	0.44	0.6880
ML	0.00020252	0.00318142	0.0995526	0.1447	0.4862

ior of reconstituted Bothkennar Clay in oedometric conditions quite well (see value of objective function in Table 8). Table 8 indicates also that the residuals of the ML model seem to be almost independent while having almost zero mean and a low skewed distribution in contrast to the other models.

6 GEOTECHNICAL BOUNDARY PROBLEM

The geotechnical boundary problem, which is treated here, is an embankment over a floating stone column reinforced foundation in Klagenfurt, Austria. The field around the stone columns is well instrumented by the Technische Universität Graz, Institute for Soil Mechanics and Foundation Engineering [22, 23]. The columns provide an increase of stiffness and strength in the treated zone and speed up the consolidation time in the upper part of the soft soil layer (lacustrine clay), which is under 11 m of loose medium dense sand.

For the identification purpose there are measurements from multilevel-piezometers, multilevel-extensometers and horizontal inclinometer. Based on the simulation of the embankment with the stone columns in 2D-, 3D- FE-Model (Fig.9) the identification of the constitutive parameters will be carried out in the same manner as for the experimental tests that is by minimizing the absolute error between measurement and numerical curves. An assortment of the conditioned

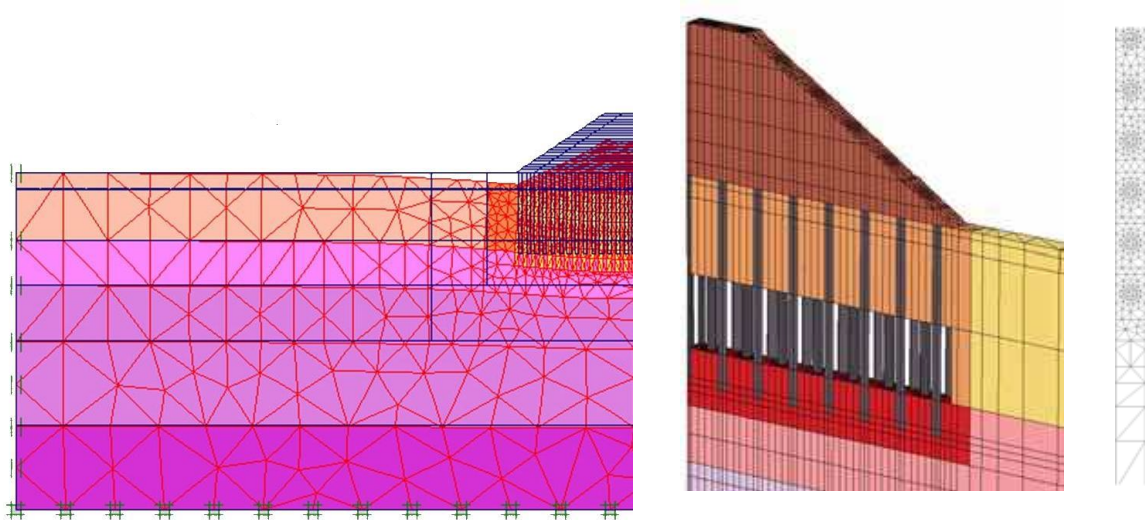


Figure 9: Different discretization Project Klagenfurt (left) 2D-model; (right) 3D-model

measurement data for the identification procedure is presented in Fig.10. Surface settlements and excess pore water pressure in different depths of 18 m, 20 m and 25 m are taken into account for the identification.

The first thirty five days of the excess pore water pressure measurement are disregarded, because the high pore water pressure is caused by the vibration of the construction of the stone columns and can not be considered in a static calculation. An increase in pore water pressure after 450 days was caused by the construction of a new structure, which is not taken into account in the FE-simulation.

The first results of the optimization for the MC model can be seen in Fig.11.

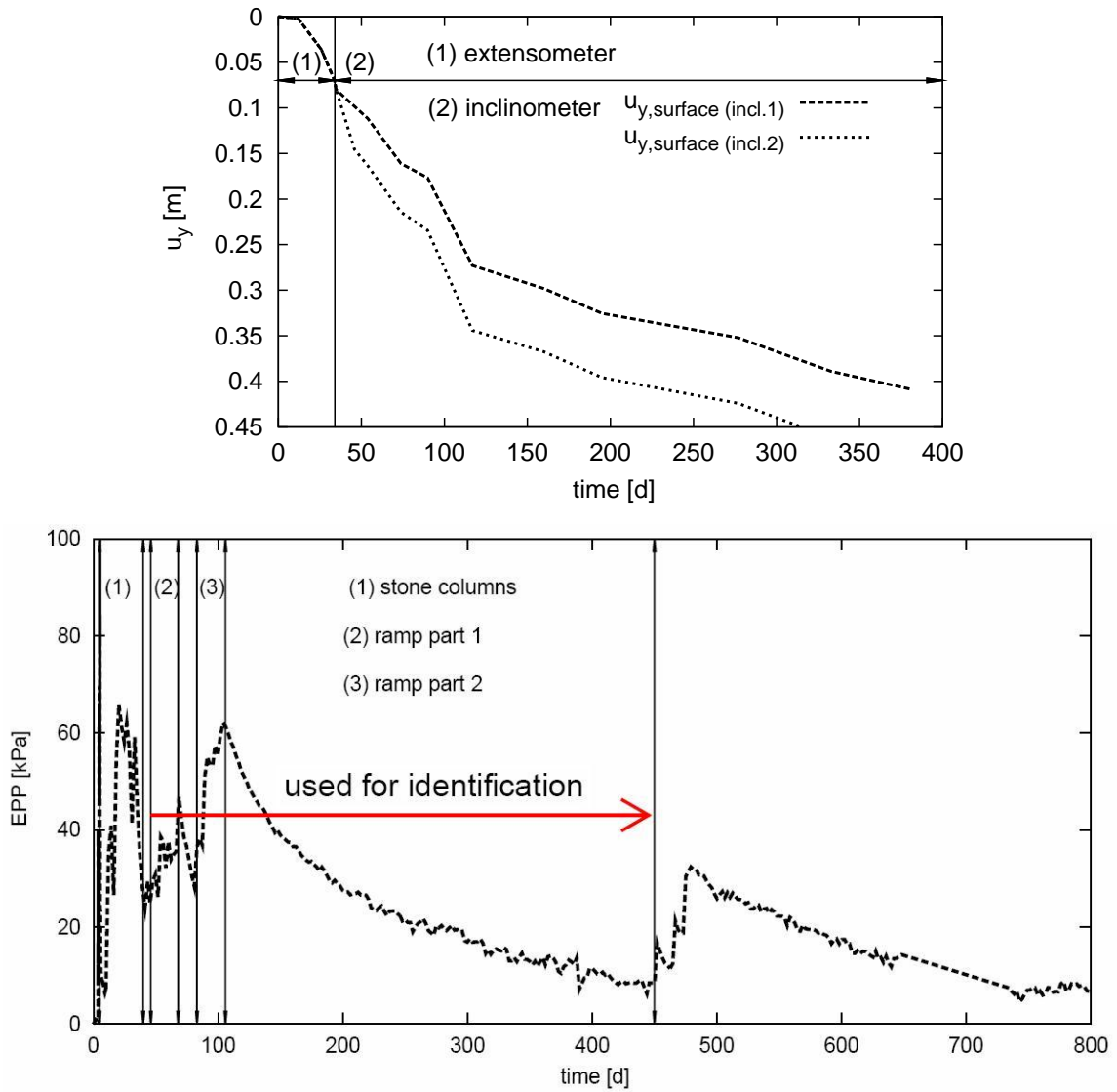


Figure 10: (above) Settlement on the surface; (below) Excess pore water pressure (18m depth) (according to [22])

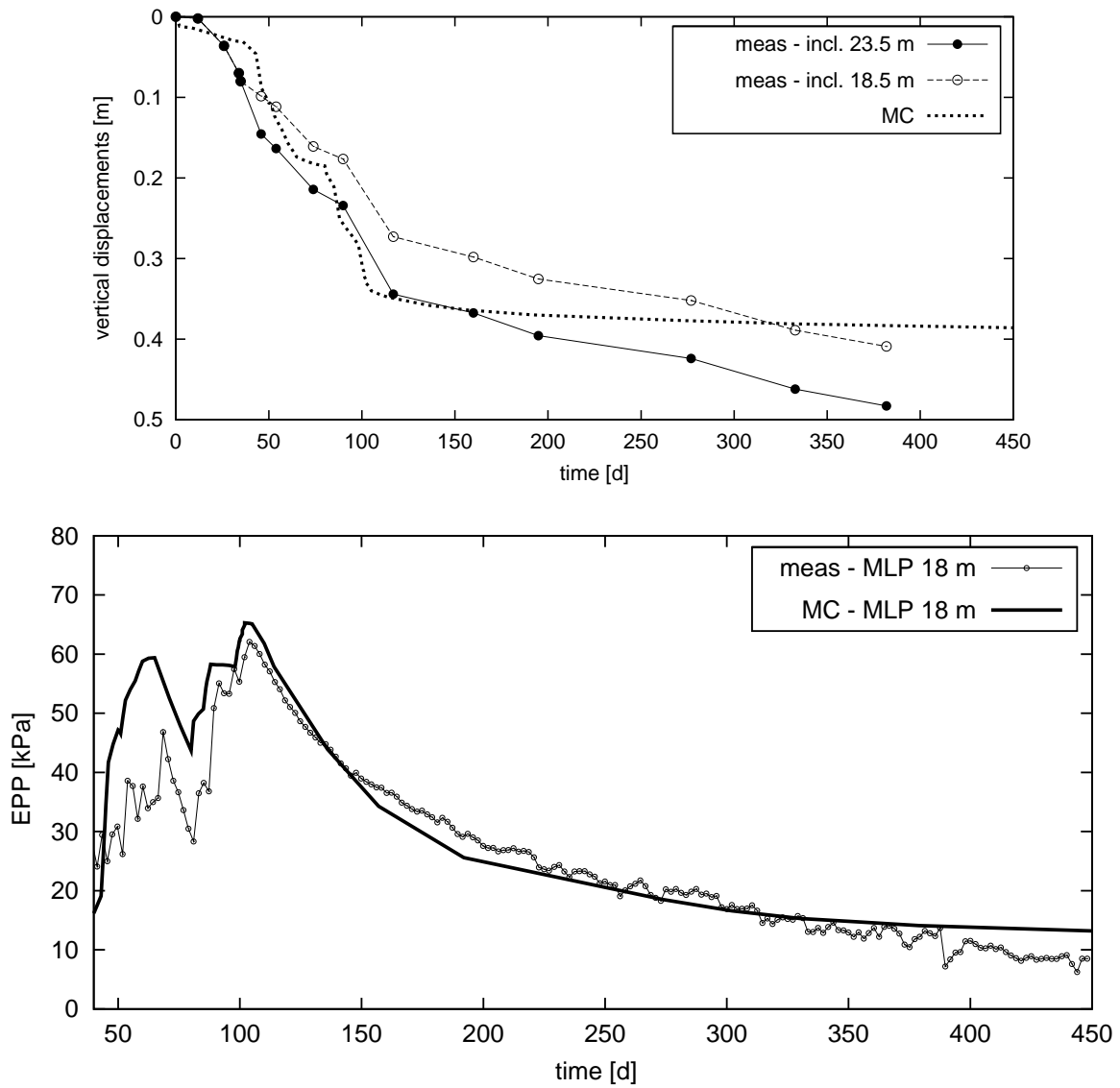


Figure 11: Results of the identification of the MC model (above) Settlement on the surface; (below) Excess pore water pressure e. g. at 18 m depth

7 CONCLUSIONS & OUTLOOK

The description of complex behavior of clay requires advanced constitutive models where is a large number of unknown constitutive parameters. Thus an efficient identification "by hand" becomes quite difficult for most practical problems. Due to the complex problems a back analysis in terms of direct or inverse approaches is used. For different laboratory tests it is possible to get good results of constitutive parameter sets.

Using statistical analysis it can be shown, that the ML model provides the best fit for the stress-strain curve on reconstituted Bothkennar Clay.

For the triaxial test on natural Bothkennar Clay the S-SCLAY and ML model can be predict the the stress-strain behavior best. Separated optimization indicates a better result of "fitting" than a simultaneous identification. This result can be attributed to sampling disturbance. Also measurement errors contribute to various test results. Furthermore, it can be detected that not all parameters can be identified equally well.

In a next step we would like to investigate a typical coupling of models structural engineering consisting of a structure and a model for the soil, e.g. a water tower on a soft soil. Whereby the soil is simulated by a partial model as a half-space with its different phenomena. The results of the identification of the element tests and the geotechnical boundary problem will help to analyze the influence of the partial model "soil" and the different complex constitutive models respectively on the calculation results (i.e. section force, energy, damage) of the coupled global model.

REFERENCES

- [1] S. J. Wheeler, M. Cudny, H. P. Neher, and C. Wiltschko. Some developments in constitutive modeling of soft clays. In *International Workshop on Geotechnics of Soft Soils-Theory and Practice*, 2003.
- [2] P. A. Vermeer and R. de Borst. Non-associated plasticity for soils, concrete and rock. *Heron*, 29, 1984.
- [3] H. P. Neher. *Zeitabhängiges Materialverhalten und Anisotropie von weichen Böden - Theorie und Anwendung*. PhD thesis, Universität Stuttgart, 2008.
- [4] M. Koskinen, M Karstunen, and S.J. Wheeler. Modeling destructuration and anisotropy of a natural soft clay. In Philippe Mestat, editor, *Proc. of the 5th European Conf. on Numerical Methods in Geotechnical Engineering, Paris*. Press de l'ENPC/LCPC, 1992.
- [5] J. Jaky. The coefficient of earth pressure at rest. *Hungarian J. Soc. Hung. Eng. Arch.(Magyar Mernok es Epitesz-Egylet Kozlonye)*, 1:355–358, 1944.
- [6] V. Galavi. *A Multilaminate Model for Structured Clay incorporating Inherent Anisotropy and Strain Softening*. PhD thesis, Technische Universität Graz, 2007.
- [7] G. N. Pande and K. G. Sharma. Multilaminate model of clays - a numerical evaluation of the influence of rotation of principal stress axes. *Int. J. of Numerical and Analytical Methods in Geomechanics*, 7:397–418, 1983.
- [8] S. Pietruszczak and Z. Mroz. Formulation of anisotropic failure criteria incorporating a microstructure tensor. *Computers and Geotechnics*, 26:105–112, 2000.

- [9] L. Callisto, A. Gajo, and D. Muir Wood. Simulation of triaxial and true triaxial tests on natural and reconstituted pisa clay. *Géotechnique*, 52:649–666, 2002.
- [10] Kabbaj M. Tavenas F. Leroueil, S. and R. Bouchard. Stress-strain-strain rate relation for the compressibility of sensitive natural clays. *Géotechnique*, 35:159–180, 1985.
- [11] F. Cotecchia. *The effects of structure on the properties of an Italian Pleistocene clay*. PhD thesis, University of London, 1996.
- [12] F. Cotecchia and R. J. Chandler. The influence of structure on the pre-failure behavior of a natural clay. *Géotechnique*, 47:523–544, 1997.
- [13] G. Baldi, D.W. Hight, and G.E. Thomas. State-of-the-art paper, a re-evaluation of conventional triaxial test methods. *Advance Triaxial Testing of Soil and Rock*, ASTM STP 977:219–263, 1988.
- [14] Jiraroth Sukolrat. *Structure and destrucuration of Bothkennar clay*. PhD thesis, University of Bristol, 2007.
- [15] K. McGinthy, M. Karstunen, and S.J. Wheeler. Modelling destructuration and anisotropy of bothkennar clay. In M. Karstunen and M. Leoni, editors, *Geotechnics of Soft Soils*, pages 263–268. Karstunen and Leoni, London, 2008.
- [16] D. W. Hight, A. J. Bond, and J. D. Legge. Characterization of the bothkennar clay: an overview. *Géotechnique*, 42:303–544, 1992.
- [17] A. L. Cividini, L. Jurina, and G. Gioda. Some aspects of characterization problems in geomechanics. *Int. J. Roc Mech. Min. Sci. and Geomech.*, 18:487–503, 1981.
- [18] J. Kennedy and R.C. Eberhard. Particle swarm optimization. In USA Publishing company Piscataway, NJ, editor, *Proc. of IEEE Int. Conf. on Neural Networks*, 1995.
- [19] T. Knabe, M. Zimmer, T. Most, and S. Schanz. Identification of constitutive parameters for geomaterials modeling using an optimization strategy. 2009.
- [20] A. Ledesma, A. Gens, and E. E. Alonso. Estimation of parameters in geotechnical backanalysis - I. Maximum likelihood approach. *Computers and Geotechnics*, 18(1):1–27, 1996.
- [21] D.C. Montgomery and G.C. Runger. *Applied statistics and probability for engineers, Third edition*. John Wiley & Sons, 2003.
- [22] M. Gäb, H.F. Schweiger, R. Thurner, and D. Adam. Field trial ti investigate the performance of a floating stone column foundation. In *European Conference on Soi Mechanics and geotechnical Engineering*, 2007.
- [23] M. Gäb, H.F. Schweiger, R. Thurner, and D. Adam. Numerical analysis of a floating stone column foundaion using different constitutive models. In Karstunen and Leoni, editors, *Geotechnics of Soft Soils- Focus on Ground Impreovement*.